arXiv:1403.5186v1 [physics.atom-ph] 20 Mar 2014

The Phase-Amplitude representation of a wave function revisited

George Rawitscher

Physics Department, University of Connecticut, Storrs, CT 06269

Abstract

The phase and amplitude (PhA) of a wave function vary slowly and monotonically with distance, in contrast to the wave function that can be highly oscillatory. Hence an attractive feature of the PhA is that it requires far fewer meshpoints than for the wave function itself. However, Milne's PhA equations contain a nonlinear term that poses numerical difficulties for conventional finite difference methods. An iterative procedure for solving Milne's equations that is very stable and converges quickly has been given by Peach and Seaton in 1962 (Proc. Phys. Soc. **79,** 1296). This method has now been implemented, combined with a spectral expansion method invloving Chebyshev polynomials. The expansionrequires very few basis functions, and equivalently, very few mesh points. In a numerical example for which the potential decreased slowly with distance as $1/r^3$, only 17 meshpoints sufficed to span a radial range of $[0, 3000]$. The resulting accuracy for the wave function was found to be of the order of a few % . This approach is expected to provide an efficient method a) to calculate wave functions out to large distances, b) to require little memory for storing wave functions, and c) for the calculation of overlap integrals that occur in many applications of quantum mechanics.

I. INTRODUCTION

When the Phase-Amplitude (PhA) method was first introduced by Milne in 1930 [1] , and then taken up by many authors, see Ref. [2], the main motivation was the paucity of numerical mesh points required, compared to the calculation of the wave function itself. This is because both phase and amplitude functions are monotonic and slowly varying, as opposed to the wave function itself that can be highly oscillatory. This point was verified by many authors, in particular by Calogero and Ravenhall [3] who state that the solution for the phase is more stable than the solution of the wave function. An additional argument in favor of the (PhA) representation is that it lends itself to analytic expressions that permit the incorporation of the effect of long range potentials [4], [5] or the calculation of resonances [2], the quantum defect of atomic wave functions [6], the calculation of Gaunt Factors [7], as well as the description of an electron with an ion embedded in a plasma [8], among others. The PhA description of a carrier wave in radio or television also plays a significant rôle in the compactification of the signal transmission in the field of Information Technology.

The PhA representation consists in writing a wave function $\psi(r)$ in the form

$$\psi(r) = y(r)\sin[\phi(r)], \tag{1}$$

where y is the amplitude and ϕ is the phase, and r the distance from the origin. Because y and ϕ vary slowly with distance, the solution of Milne's equation can be done on a very small number of radial mesh points (17 to 33, as shown below), particularly if both y and ϕ are obtained by means of a spectral representation [9]. If an overlap matrix element

$$M = \int_0^\infty \psi_1(r)U(r)\psi_2(r)dr. \tag{2}$$

between two wave functions is required, then in the finite difference method of obtaining integrals, both ψ_1 and ψ_2 have to be calculated on a sufficiently fine mesh, which can be time consuming and prone to errors. However, the PhA representation can provide an estimate of $M_{1,2}$ by decomposing the integrand of such an overlap matrix element into a slowly oscillating (S) and a fast oscillating (F) part

$$M = M^{(S)} - M^{(F)}. \tag{3}$$

The decomposition makes use of a trigonometric identity for the product of two sine functions

with the result

$$M^{(F,S)} = \frac{1}{2}\int_0^\infty y_1(r)U(r)y_2(r)[\cos(\phi_1 \pm \phi_2)]dr. \tag{4}$$

The matrix element $M^{(S)}$ can be calculated on the small spectral mesh since the integrand oscillates slowly, and since $M^{(F)} \ll M^{(F)}$, an estimate for M is provided by $M^{(S)}$. In addition, for calculations that require the storage of many wave functions with high precision [10] the amount of storage required can be substantially reduced by means of the use of the spectral PhA representation, because the latter can be interpolated to any desired set of mesh-points.

It is the purpose of the present work to demonstrate the viability and accuracy of the calculation of the phase and amplitude, and hence of the wave function. The method solves Milne's nonlinear differential equation for the amplitude [1] by an iteration procedure introduced in 1962 by Seaton and Peach [11], and implemented here by an Chebyshev spectral expansion method [9]. The novel aspects of the present work are a) implementing Seaton and Peach's iterative solution [11] of Milne's equation [1] by an efficient spectral method, and b) examining the accuracy of the Phase Amplitude result by comparison with the solution of the Schrödinger equation for the wave function, the latter obtained by an accurate spectral integral equation method [12], denoted as IEM in what follows.

In section II the iterative method is explained, section III contains details of the computational spectral method, section IV presents the results, including error estimates and suggestions for improvements, and finally the Summary and Conclusions are presented in section V.

II. ITERATIVE SOLUTION OF MILNE'S PHASE-AMPLITUDE EQUATION.

Milne [1] and others have derived a non linear equation for the amplitude y and phase ϕ, the latter defined in Eq. (1), which is

$$y'' + k^2 y = V_T\ y + \frac{k^2}{y^3} \tag{5}$$

where the total potential V_T is

$$V_T = L(L+1)/r^2 + V(r). \tag{6}$$

Here $V(r)$ is the atomic or nuclear potential (including the Coulomb potential), L is the orbital angular momentum quantum number, and the nonlinearity is given by the last term

in Eq. (5). The phase $\phi(r)$ is obtained from the amplitude $y(r)$ according to

$$\phi(r) = \phi(r_0) + k \int_{r_0}^{r} [y(r')]^{-2}\, dr', \tag{7}$$

but it can also be obtained without the knowledge of y [7]. The Eq. (5) has been solved non-iteratively in the past by using some form of a finite difference computational method, such as one of Milne's predictor-corrector methods [13], or [8] by a Bulirsch-Stoer limit method [14]. Alternatively, the iterative method of Seaton and Peach [11] consists in rewriting Eq. (5) in the form

$$\frac{k^2}{y^4} = w + \frac{1}{y}\frac{d^2y}{dr^2} \tag{8}$$

where

$$w(r) = k^2 - V_T, \tag{9}$$

and calculating the solution of Eq. (8) by the iteration [11]

$$\frac{k}{y_{n+1}^2} = [w + \frac{1}{y_n}\frac{d^2y_n}{dr^2}]^{1/2}, \quad n = 0, 1, 2, ... \tag{10}$$

Here n denotes the order of the iteration, and the initial value of y is given by the WKB approximation [15]

$$\frac{k}{y_0^2} = w^{1/2}. \tag{11}$$

For each iteration the resulting amplitude y is normalized to unity at a suitable asymptotic distance. The advantage of formulating the iteration according to Eq. (10) is that y varies slowly and monotonically with r for large distances, and hence $(1/y_n)d^2y_n/dr^2$ is small compared to w . Near the origin of r this term becomes large, but a numerical solution of Eq. (10) still converges very well as shown below, in agreement with the finding of Ref. [11].

III. COMPUTATIONAL METHOD

The computational method consist in expanding the amplitude y into a series of $N+1$ Chebyshev Polynomials $T_s(x)$, $s = 0, 1, 2, ..N$. That expansion is inserted into Eq. (10), and the corresponding coefficients a_s

$$y(x) = \sum_{s=0}^{N} a_s T_s(x) \tag{12}$$

are obtained by solving a matrix equation [12], [16]. Since the Chebyshev polynomials are defined in the interval $-1 \leq x \leq 1$ the quantities defined in the radial interval $r_0 \leq r \leq r_{\max}$ are mapped into the $x-$variable by a linear transformation. The x- mesh points are the $N+1$ zeros of T_{N+1}. The expansion cutoff value of N is set arbitrarily, but once chosen, the location and number of support points on the $x-$axis is determined. Extensive use is made of Clenshaw-Curtis matrix expression (CC) [17] that relates the values of a function evaluated at the $N+1$ mesh-points to the expansion coefficients a_s of that function, and vice-versa. The nonlinearity aspect of Eq. (10) is overcome as follows. First the expansion coefficients a_s arising from the known right hand side of Eq. (10) are obtained. In terms of these the values of k/y_{n+1}^2 at the mesh points can be obtained via the CC relations, and hence the values of y_{n+1} at these mesh points can be obtained by taking square roots. The corresponding expansion coefficient for y_{n+1} are obtained again by using the CC relations, and the iteration can proceed. However the calculation of the second order derivative in Eq. (10) introduces errors [16], and these errors increase as N is made larger. This feature is the major source of error in the present procedure, since the Chebyshev polynomials do not lend themselves well for obtaining derivatives, as shown below. The integral in Eq. (7) required to calculate the phase ϕ is performed by a Gauss Chebyshev method [12], [16] that is well suited to this type of spectral expansion.

The calculations are done with MATLAB on a desk PC using an Intel TM2 Quad, with a CPU Q 9950, a frequency of 2.83 GHz, and a RAM of 8 GB. The calculation that uses $N+1 = 17$ Chebyshev polynomials for the calculation of y, subsequently interpolated to 33 polynomials for the calculation of the phase ϕ, is denoted as $(16-32)$ in the text. The computing time for that part of the calculation, including performing 4 iterations, requires between 0.3 s and 0.4 s, regardless of the size of the radial interval. Interpolating y and ϕ to an equi-spaced radial mesh size of step length $h = 0.1$ requires an additional 170 s to 180 s for a radial interval $[0, 3000]$, or 0.8 s for the radial interval $[0, 40]$. However, the calculation of the slowly oscillating part $M^{(S)}$ of an overlap matrix element (4) can be done without interpolating to an equi-spaced radial mesh, by using the Gauss-Chebyshev integration method [16], and is expected to take approximately 1 s to 2 s for obtaining each of the two wave functions, and subsequently calculating $M^{(S)}$.

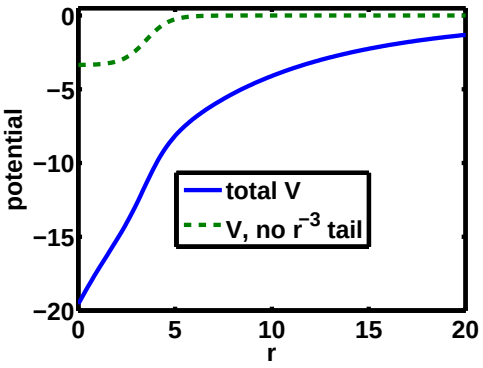

FIG. 1: The solid line illustrates the potential used for the numerical example. The units are in inverse length squared, since the potential in energy units has been multiplied by the factor $2m/\hbar^2$. The dashed line indicates the Woods-Saxon potential to which is added a $1/r^3$ "tail", as described in the text.

IV. RESULTS

The feasibility of the present approach will be demonstrated by means of an example, for which the potential V_T is everywhere attractive and has a long range tail proportional to r^{-3}. The wave number is $k = 0.01$, the radial region extends from $r = 0$ to $r = 3000$, and the orbital angular momentum is $L = 0$. In Eq. (5) the factor $\hbar^2/2m$ has already been divided into the potential and into the energy k^2, so that both are given in units of inverse distance squared. The unit of distance can be either fm for nuclear physics applications, or the Bohr radius a_0 for atomic physics applications, but will not be explicitly indicated.

The potential is the sum of a Woods-Saxon form, Eq. (13), to which is added a r^{-3} tail, whose singularity at the origin is smoothly removed by an analytic mapping procedure, Eqs. (14-15)

$$V_{WS}(r) = -3.36 \ / \ [1 + \exp\{(r - 3.5)/0.6\}] \tag{13}$$

$$V_3(r) = -1.6224 \times 10^4/\mathcal{R}^3 \tag{14}$$

$$\mathcal{R}(r) = r/[1 - \exp(-r/10)] \tag{15}$$

$$V = V_{WS} + V_3 \tag{16}$$

The Woods Saxon part and the total potential V are illustrated respectively by the dashed and solid lines in Fig. 1. The long-ranged nature of this potential is illustrated in Fig.

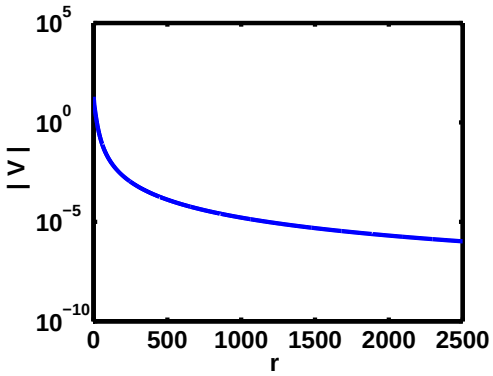

FIG. 2: Illustrated here is the long range extent of the potential used for the numerical calculation.

.

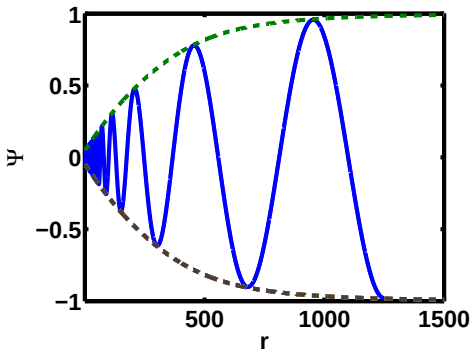

FIG. 3: Comparison of the amplitude y, illustrated in Fig. 4, and shown here by the dashed lines, with the solid line representing the IEM wave function. This figure shows that the extrema of the wave function visually coincide with the amplitude values.

2. At $r = 2500$ the value of V is $\simeq 10^{-6}$, and at this point the values of y_n for each n are normalized to unity. The corresponding wave function is highly oscillatory at small distances, with an amplitude that varies substantially with distance, as is illustrated in Fig. 3. The corresponding amplitude is illustrated in Fig. 4, for various iteration orders n, and also by the dashed lines in Fig. 3. Noteworthy is the fact that only 17 expansion terms in Eq. (12) have been used to cover the whole radial interval $[0, 3000]$. Unless otherwise noted, the numerical results described further below are carried out to the third iteration order $n = 3$.

This amplitude is in good agreement with the wave function calculated by the spectral

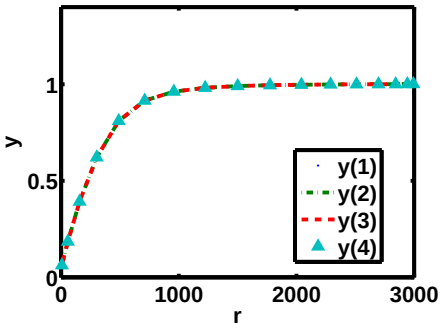

FIG. 4: The values of the amplityde y, solution of the Milne Eq. (10) using the Chebyshev expansion (12) with 17 terms (i.e., $N = 16$). The corresponding 17 mesh points cover the whole radial interval $[0, 3000]$. The number of iterations n is denoted by the numbers in parenthesis in the legend.

IEM method [12], denoted as IEM, as shown in Fig. 3. The corresponding phase ϕ, based on Eq. (7), is illustrated in Fig. 5. However, the number 17 of basis functions, sufficient for the amplitude calculation, is insufficient to perform the integral in Eq. (7), as is illustrated in Fig. 5 by the non-monotonic behavior of the dash-dotted line. In order to increase the number of Chebyshev polynomials, the expansion (12) was interpolated to 33 mesh points, and the corresponding result for ϕ is illustrated in Fig. 5 by the line with triangles. The wave function calculated in terms of the phase and amplitude according to Eq. (1), denoted by "PhA" in Fig. 6, uses for both y and ϕ the 33 basis functions. The result is in good agreement with the IEM wave function for radial distances $r < 50$. However the agreement deteriorates for the larger distances, due to the accumulation of an error in the phase..

In order to examine the phase error in more detail, the calculation was repeated for a smaller radial domain $0 \leq r \leq 40$ with 17 expansion Chebyshev functions for the amplitude in that domain. That number is augmented to 33 by interpolation, and the corresponding phase ϕ is calculated by means of Eq. (7). Good agreement to within 1% with the IEM wave function is obtained, as shown by the solid line in Fig. 7. When a small ad hoc additional phase of 0.03 π radians is added to the phase, the agreement with the IEM wave function is improved, as shown by the dashed line in Fig. 7. If the calculation in the radial interval $[0, 40]$ is repeated with an initial number of Chebyshev functions increased from 17 to 21, the error in the phase amplitude wave function increases, as illustrated in Fig. 8 by the dashed

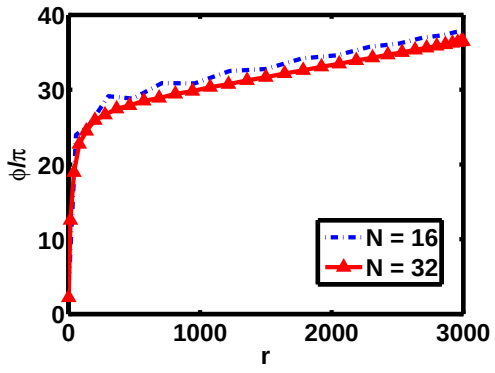

FIG. 5: The phase ϕ at the Chebyshev support points. The $N = 16$ line illustrates the result obtained by evaluating the integral (7) using the total 17 meshpoints for y. The $N = 32$ line gives the result if the amplitudes for $N = 16$ are first interpolated to $N = 32$ before doing the integral .

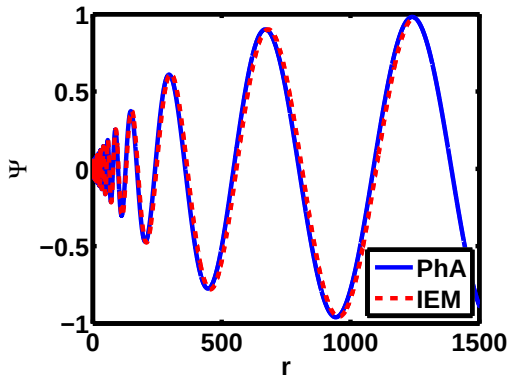

FIG. 6: The solid line, labelled PhA, represents the wave function calculated from Eqs. (1) with y obtained from the third order iterated Eq. (5), with $N = 16$, and the phase ϕ obtained from Eq. (7) with the values of y first interpolated from the $N = 16$ values to $N = 32$. The dashed line labeled IEM is obtained by solving the Schrödinger equation directly with the IEM method.

line. An investigation not shown here confirms that the error is introduced when calculating the derivative of the function y_n in Eq. (10). In order to show that a slight phase error continues to aggregate for larger distances, the phase amplitude calculation was repeated in the domain $[40 \leq r \leq 2500]$, using for $\phi(r_0)$ the phase obtained from the calculation in the radial domain $[0, 40]$, augmented by the additional value $0.03\ \pi$. The result is shown in Figs. 9 and 10.

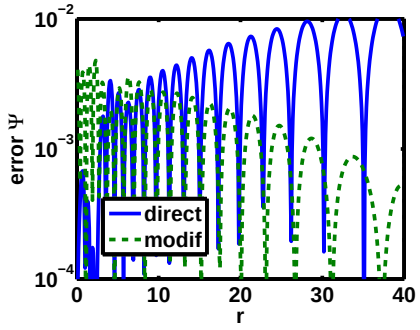

FIG. 7: The y-axis shows the absolute value of the difference between the PhA and IEM wave functions. The PhA wave function, defined in Eq. (1) is obtained with y calculated with 17 mesh points in the radial interval $[0, 40]$, and interpolated to 33 meshpoints, in terms of which ϕ.is evaluated. The result is labeled "$direct$" in the legend. The result labeled "$modif$" is obtained by adding the additional constant 0.03π to the "$direct$" value of ϕ.

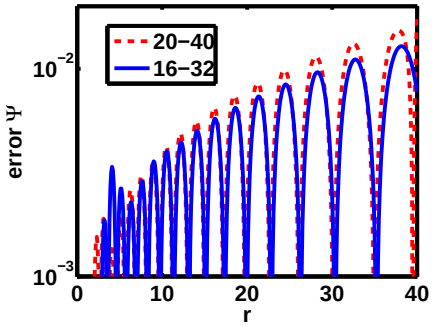

FIG. 8: The error of the PhA wavefunction labeled $16-22$ is the same as in Fig. 7, where it is labelled "direct". The result labeled $20-40$ uses 21 Chebyshev polynomials in the radial domain [0,40], subsequently interpolated to 41 polynomials for the calculation of ϕ. The graph shows that the error in the phase increases with an increased number of basis functions.

The general conclusion from the above results is that the main error is due to the use of Chebyshev polynomials in the expansion (12), rather than using a different set of basis functions that lend themselves to a more accurate calculation of the second order derivatives in Eq. (10). Such an investigation will be carried out in a future study.

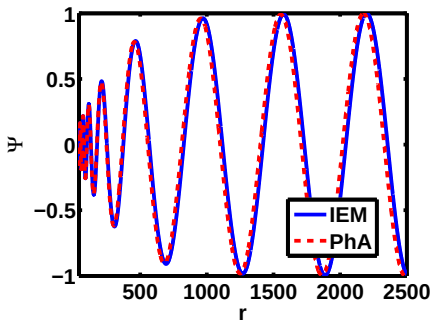

FIG. 9: Comparison of the PhA and IEM wave functions in the radial interval $[40, 2500]$. The PhA function is obtained with 17 basis functions for y, subsequently interpolated to 33. The phase is calculated with the 33 y values, and the additive constant for the phase at $r = 40$ is obtained from the phase of the function illustrated by the dashed line in Fig. 7.

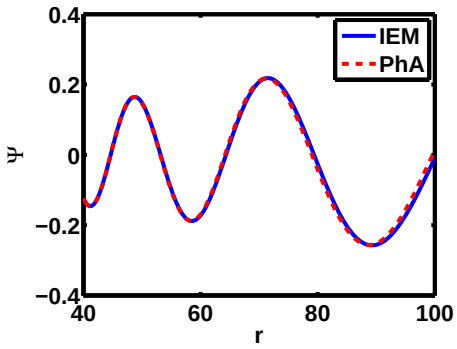

FIG. 10: Same as Fig 9, plotted in the smaller radial domain [40,100].

A. Overlap Integrals

An example of the calculation of matrix elements by means of the PhA method will be presented below. The two wave functions ψ_1 and ψ_2 are solutions of the one-dimensional radial Schrödinger equation with the potential V defined in Eqs. (13) to (16), for different wave numbers $k = 0.01$ and 0.005, respectively (in units of inverse length). The two wave functions have different amplitudes, but nearly the same phases at distances where $|V| > k^2$, as is illustrated in Fig. 11. Potential U is given in Eq. (4) of Ref. [8], and represents the screened interaction of an electron with an ion embedded in a plasma. It is composed of a sum of exponentials divided by the radial distance r, and is illustrated in

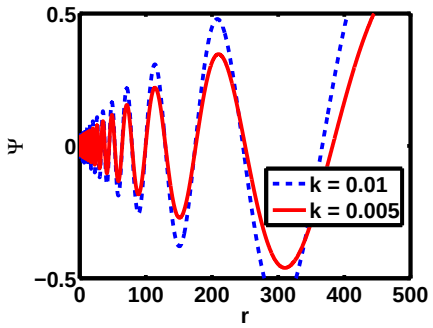

FIG. 11: The two wave functions used for the calculation the matrix element M defined in Eq. (2). Both functions have unit amplitude at $r = 2500$.

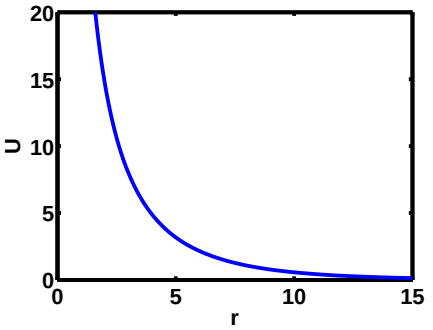

FIG. 12: The potential U that occurs in the matrix element M, defined in Eq. (2). Because of the factor $1/r$, it becomes ∞ at $r = 0$. The units of U are $(1/length)^2$

Fig.12. Using the PhA representation of ψ_1 and ψ_2, the integrand of the overlap integral separates into a fast oscillating and slowly oscillating parts, Eqs. (4). These integrands are illustrated in Fig. 13. The approximate values of $M^{(F)}$and $M^{(S)}$ are -0.073 and 0.258. As expected, the integrand of $M^{(F)}$ is much more oscillatory than the integrand of $M^{(S)}$, and hence $|M^{(F)}| < |M^{(S)}|$.

V. SUMMARY AND CONCLUSIONS

An effective method was developed to solve the nonlinear equations of Milne for the amplitude and phase of a wave function. The method consists in combining the iteration scheme, developed in the sixties by Seaton and Peach [11], with a spectral expansion of

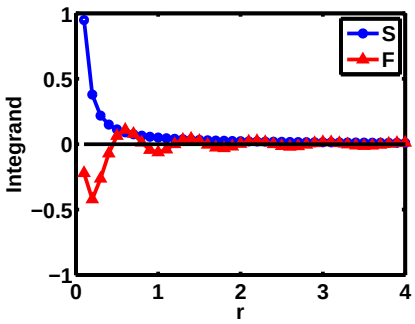

FIG. 13: The integrands of the matrix elements $M^{(F)}$ and $M^{(S)}$. Due to the rapid oscillation of the integrand of $M^{(F)}$, it is clear that $M^{(F)} < M^{(S)}$.

y. The spectral basis set for the expansion of y consisted of Chebyshev polynomials, that are especially convenient for carrying out the integrals contained in the equations. For a numerical example that contains a long range potential tail of the r^{-3} form, it was found that 17 basis functions sufficed to span the entire radial domain from the origin to $r = 3000$ with good accuracy for the amplitude. The calculation of the phase was most sensitive to the numerical errors, an accuracy of several percent was nevertheless achieved for the wave function. The errors were examined by comparison to the solution of the Schrödinger equation obtained by a spectral method [12], whose accuracy has been tested previously. Future improvements will consist in examining other sets of spectral basis functions that are more convenient for calculating the second order derivatives that occur in the iterative scheme, given by Eq. (10).

The method is expected to be very useful for a) the calculation of overlap matrix elements that involve highly oscillatory wave functions, b) to obtain the long range value of wave functions in cases where the conventional solutions of the Schrödinger equation may be inadequate, and c) also to provide a very economical method to store wave functions via the PhA representation.

The author is indebted to Dr. Ionel Simbotin for calling attention to the PhA representation, and for stimulating conversations.

---

[1] W. E. Milne, Phys. Rev. **35**, 863 (1930);

[2] M. J. Korsch and H. Laurent. J. Phys. B: At. Mol. Phys **14,** 4213 (1981);

[3] F. Calogero and D. G. Ravenhall, Nuovo Cimento **32**, 1755 (1964);

[4] F. Robicheaux, U. Fano, M. Cavagnero, and D. A. Harmin, Phys. Rev. A, **35**, 3619 (1987);

[5] J. L. Dehmer and U. Fano, Phys. Rev. **A 2**, 304 (1970);

[6] C. H. Greene, A. R. P. Rau and U. Fano, Phys. Rev. **A 26**, 2441 (1982);

[7] B. Wilson, C. Iglesias, and Mau Chen, J. Quant. Spectrosc. Radiat. Transf. **81**, 499 (2003);

[8] A. B. Ritchie and A.K. Bhatia, Phys. Rev. E **69**, 035402(R), 2004

[9] A. Deloff, Ann. Phys. (NY) **322**, 1373–1419 (2007);L. N. Trefethen, *Spectral Methods in MATLAB*, (SIAM, Philadelphia, PA, 2000); John P. Boyd, *Chebyshev and Fourier Spectral Methods,* 2nd revised ed. (Dover Publications, Mineola, NY, 2001);

[10] V. A. Dzuba, A. Derevianko, J. of Phys. B: Atomic, Molecular and Optical Physics, **43**, 074011 (2010); V. A. Dzuba, A. Derevianko, V. V. Flambaum, Phys. Rev. **A 86**, 054501 (2012); S. G. Porsev, A. Derevianko, Phys. Rev. **A 74**, 020502, (2006); M. S. Safronova, S. G. Porsev, U. I. Safronova, M. G. Kozlov, C. W. Clark, Phys. Rev. **A 87**, 012509 (2013);

[11] M. J. Seaton and G. Peach Proc. Phys. Soc. 79 1296 (1962) doi:10.1088/0370-1328/79/6/127

[12] R. A. Gonzales, J. Eisert, I Koltracht, M. Neumann and G. Rawitscher, J. of Comput. Phys. **134**, 134 (1997); R. A. Gonzales, S.-Y. Kang, I. Koltracht and G. Rawitscher, J. of Comput. Phys. **153**, 160-202 (1999);

[13] M. Abramowitz and I. Stegun, eds., (Handbook of Mathematical Functions, Dover, 1972), Eq. 25.5.13;

[14] W. H. Press, S. A. Teukolsky, W. T. Vetterling, B. P. Flannery, (2007). "Section 17.3. Richardson Extrapolation and the Bulirsch-Stoer Method". Numerical Recipes: *The Art of Scientific Computing (3rd ed.)*. New York: Cambridge University Press. ISBN 978-0-521-88068-8.

[15] H. Jeffreys an B. S. Jeffreys, *Methods of Mathematical Physics,* Cambridge University Press, NY (1966); H. A. Kramers, Z. Physik, **39**, 828 (1926);

[16] G. Rawitscher and I. Koltracht, Computing Sci. Eng. **7**, 58 (2005);

[17] C.C. Clenshaw, and A.R. Curtis, Numer. Math., 1960, **2,** 197;